

Fig. 1. Isolated AC-DC converter with three-phase-to-single-phase matrix converter.

commutation and another commutation method to prevent the short-circuit at the critical area. The effectiveness of the proposed two-step commutation is evaluated with a 10-kW prototype thought experimental results.

2. Circuit configuration and control method

Figure 1 shows the isolated AC-DC converter with the three-phase to single-phase matrix converter. The proposed circuit consists of a LC filter to eliminate switching ripple component of the input current, a three-phase to single-phase matrix converter with bi-directional switches, a medium frequency transformer, a diode rectifier, and a smoothing inductor in the output DC side. In particular, the three-phase grid voltage is directly converted to medium frequency single-phase voltage by the matrix converter. Consequently, the volume of the transformer is significantly minimized because this transformer is operated with this medium frequency single-phase voltage

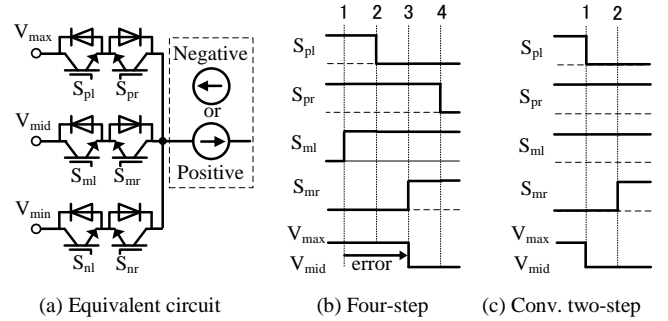
3. Two-step commutation method

3.1 Problem of conventional commutation method

Figure 2 shows the equivalent circuit at each arm of the matrix converter. The equivalent circuit consists of the three voltage sources (maximum-phase-voltage V_{max} , middle phase-voltage V_{mid} , minimum phase-voltage V_{min}), current source which represents as the current at the transformer, and three bi-directional switches. Figure 2(b) and 2(c) show the transition situation from V_{max} to V_{mid} with the four-step voltage commutation and the conventional two-step commutation. If the actual voltage polarity does not agree with the detection voltage polarity, the short-circuit via the grid occurs in the commutation state of the four-step voltage commutation or in the steady state of the conventional two-step commutation until turning-on S_{mr} .

3.2 Principle of two-step commutation

Figure 3 depicts the principle of the proposed two-step commutation, which is divided into three modes. Figure 3(a) shows the transition from the high voltage to the low-voltage. As shown in Fig. 3 (a), the switch S_{pr} turns-on at V_{max} -phase when the matrix converter starts to transit from V_{max} -phase to V_{mid} -phase with the positive output current. At first step, the switch S_{mr} at V_{mid} -phase turns-on. Then, at second step, the switch S_{pr} turns-off and the current commutates from V_{max} -phase to V_{mid} -phase. The output voltage error occurs due to the commutation from V_{max} -phase to V_{mid} -phase. Figure 3(b) shows the



(a) Equivalent circuit (b) Four-step (c) Conv. two-step

Fig. 2. Conventional commutation step. If the actual voltage does not agree with the detection voltage, the short-circuit occur by the commutation failure.

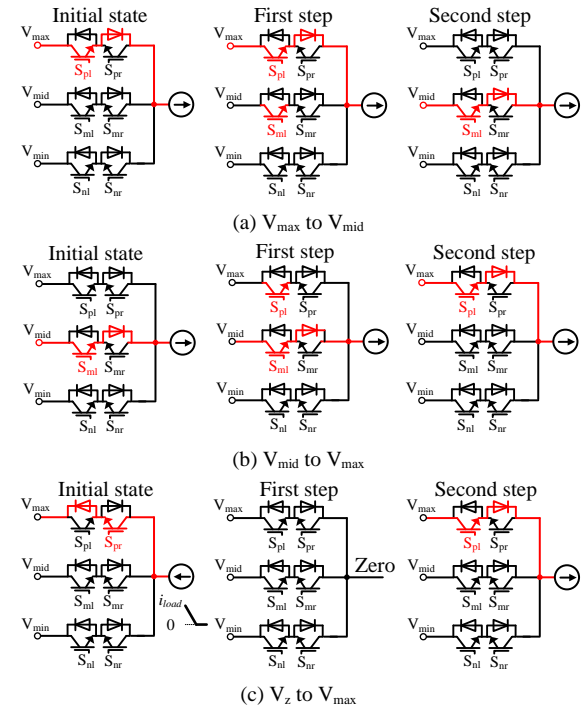


Fig. 3. Proposed commutation sequence. The commutation step is always two-step by proposed sequence.

transition from the low voltage to the high voltage. In contrast, the switch S_{mr} turns-on at V_{mid} -phase when the matrix converter starts

to transit from V_{mid} -phase to V_{max} -phase with the positive output current. At first step, the switch S_{pr} at V_{max} -phase turns-on and the current commutates from V_{mid} -phase to V_{max} -phase. Then, at second step, the switch S_{mr} turns-off. The output voltage error is zero when the output voltage is changed from V_{max} -phase to V_{mid} -phase. Figure 3(c) shows the transition from zero-vector state to an input phase. The output current decreases until zero in the initial state. After that, the output current keeps to zero because the current path is nothing regardless of the switching state of S_{pr} . Therefore, the zero-vector state V_z is defined as an equivalent off state of all switching devices of the matrix converter. The zero-vector state depend on the input voltage polarity. At first step, the all switches turn-off because the output current is already zero. At second step, S_{pl} turns-on and the output voltage is changed from zero to V_{max} . Therefore, the output voltage error should occur by the zero-vector. In this paper, the commutation from the low to high voltage is excluded to achieve the simple duty compensation because the output voltage error is always a constant duty using other commutation.

In these commutation modes, the short-circuit and the open-circuit are avoided regardless of the voltage detection error by the modulation of only one of two devices in the bi-directional switches. Therefore, the transition from an input phase to another input phase without any commutation failures is achieved. The initial state is on state of S_{pl} and then similar switching sequence are applied when the output current direction is negative. The initial state of the equivalent commutation model for each arm is express by (1)

$$\begin{cases} S_{xl} = 1 & S_{xr} = 0 & i_{load} > 0 \\ S_{xl} = 0 & S_{xr} = 1 & i_{load} < 0 \end{cases} \quad x = p, m, n \quad (1)$$

where subscript x indicates p (V_{max} -phase) or m (V_{mid} -phase) or n (V_{min} -phase) depend on the output line to line voltage V_{pr} . If the output voltage of the matrix converter is $V_{max}-V_{min}$, x of the upper side arm is p. In addition, x of the lower side arm is n.

Figure 4 shows the half-cycle operation of one switching period including commutation in sector I. The relationship of phase-voltage is $v_r > v_s > v_t$. The inductor current I_{dc} is assumed to be ideal as no ripple current.

(i) $t_0 - t_1$

S_{rp} and S_{nr} are on, whereas the output current direction is positive. Therefore, S_{rp} and S_{nr} can only conduct the current through the diode connected anti-parallel with the switching devices.

(ii) $t_1 - t_2$

S_{sp} is turned-on. The current flow does not change because the R-phase voltage is higher than the S-phase voltage.

(iii) $t_2 - t_3$

S_{rp} is turned-off. The output voltage is changed from V_{max} -phase to V_{mid} -phase. This matrix converter successfully outputs vector V_2 .

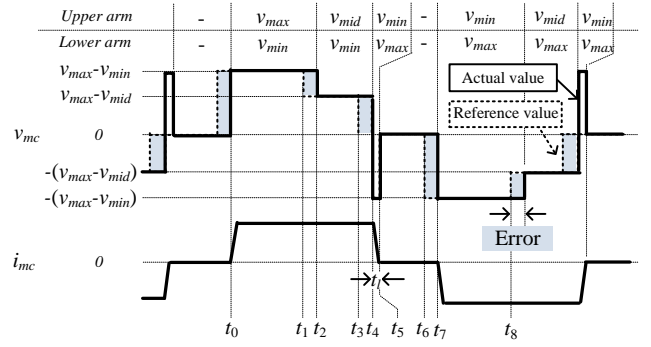
(iv) $t_3 - t_4$

S_{rp} and S_{nr} is turned-on, whereas the output current direction is still positive.

(v) $t_4 - t_5$

S_{sp} and S_{nr} is turned-off. The output voltage polarity is changed to be opposite of the output current. Thus, the output current quickly decreases to zero during t_l . The time t_l is expressed by

$$t_l = L_l \frac{I_{dc}}{Nv_{mc}} \quad (2)$$



(a) Operation waveforms at high-frequency side

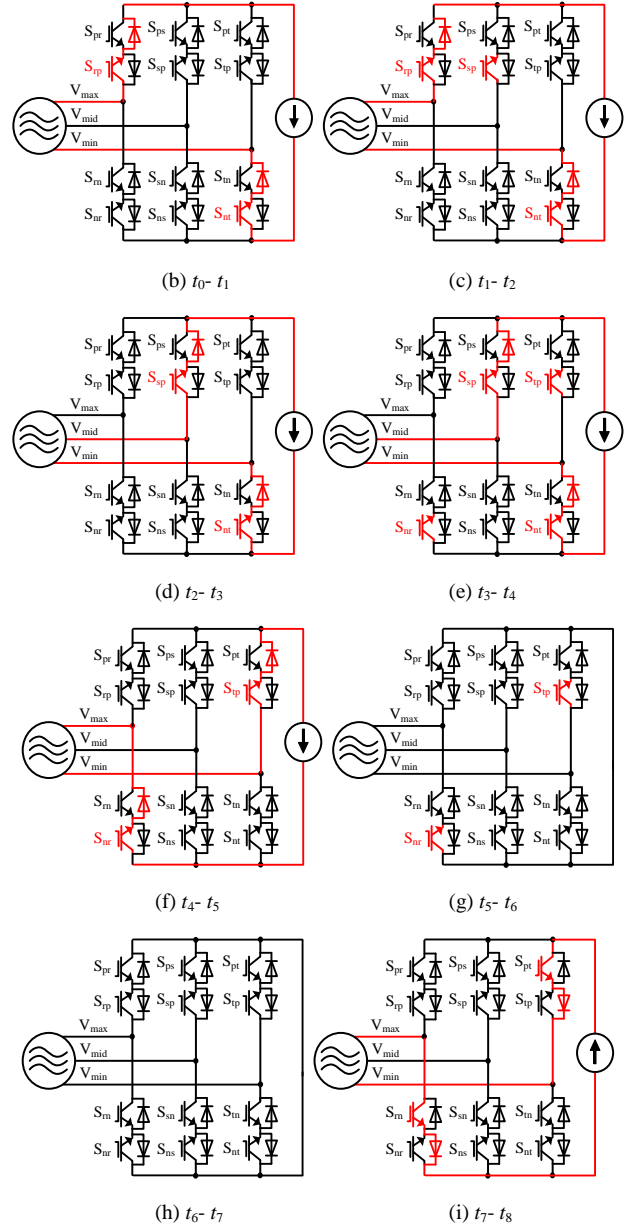


Fig. 4. Transition situation during half cycle one switching period.

where N is the turn ratio of the transformer, L_l is the leakage inductance of the transformer, v_{mc} is the single-phase output voltage, and I_{dc} is the output current at dc side. The output voltage during t_l is the line to line voltage between V_{max} -phase and V_{min} -phase to

minimize the time t_l . This output voltage during t_l is error. However, this output voltage error is ignored because this period is lower than $1/10$ of a dead-time using the small leakage inductance and the high output voltage.

(vi) $t_5 - t_6$

The output current keeps to zero regardless of the switching states of S_{tp} and S_{nr} . The output voltage is also clamped to zero because the inductor current at DC side is circulated at the diode rectifier in secondary side during zero-vector state. The commutation failure occurs by next commutation sequences when the output current is not zero. The time t_l should be shorter than zero-vector state from t_4 to t_6 to suppress the commutation failure.

(vii) $t_6 - t_7$

S_{sp} and S_{nr} can safely turned-off because the output current has become zero when the time t_l is shorter than zero-vector state.

(viii) $t_7 - t_8$

S_{rn} and S_{pt} are turned-on and the matrix converter outputs the negative voltage.

In consequence, the proposed two-step commutation operates the matrix converter without any commutation failures regardless of the detection voltage error at the input voltage.

Figure 5 shows the proposed two-step commutation sequence. The output voltage error due to the dead time is considered. The delay of one-step time occurs from the first step to the second step as shown in Fig. 2 (a) when the matrix converter transits from an input phase to another input phase in the positive output current. In the transition from the zero-vector state to another input phase, all switches have to be turned-off at the first step. Similarly, the delay of one-step time occurs from the first step to the second step as shown in Fig. 2 (b). Consequently, the compensation for the voltage error due to the delay of one-step time of the proposed two-step commutation is similar to that in the back-to-back converter, which is significantly simpler than the output voltage error compensation in the four-step commutation.

4. Circuit configuration and control method

4.1 Input current control for matrix converter Figure 6 shows the space vector modulation (SVM) applied to the three-phase to single-phase matrix converter. The operation mode of SVM is divided by every 60 deg. (Sector I, II, III, IV, V and VI) of the input voltages. Output vectors which are close to the input voltage vector are selected. In sector I, V_1 and V_2 are used during the first half of the control period as the positive voltage, whereas V_4 and V_5 are used during the second half of the control period as the negative voltage. Note that the zero vector V_z which outputs the zero voltage, is decided by the sector. These duty reference T_1 , T_2 , and T_z are calculated by

$$T_1 = \frac{1}{|A|} \begin{vmatrix} v_\alpha & V_{2\alpha} \\ v_\beta & V_{2\beta} \end{vmatrix} \quad (3)$$

$$T_2 = \frac{1}{|A|} \begin{vmatrix} V_{1\alpha} & v_\alpha \\ V_{1\beta} & v_\beta \end{vmatrix} \quad (4)$$

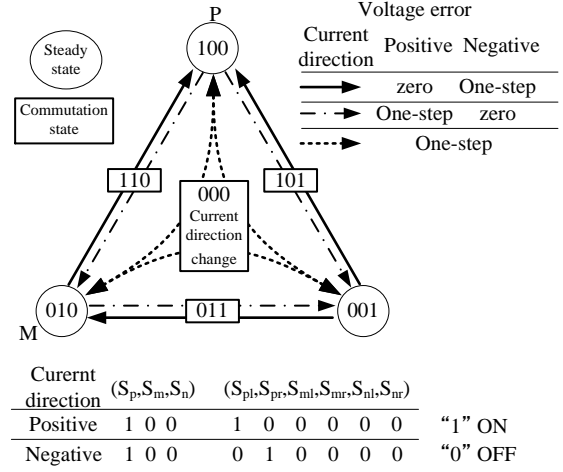
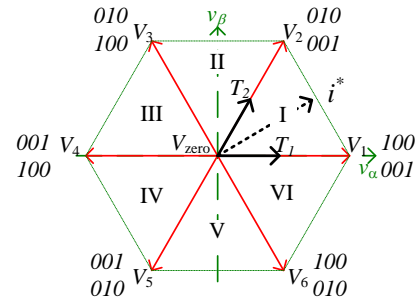


Fig. 5. Proposed two-step commutation sequence.



※ The number of "1" means switch is Turn on
 Example $\begin{cases} 100 & S_{rp}' = \text{ON}, S_{sp}' = \text{OFF}, S_{tp}' = \text{OFF} \\ 001 & S_{rn}' = \text{OFF}, S_{sn}' = \text{OFF}, S_{tn}' = \text{ON} \end{cases}$

Fig. 6. Space vector modulation.

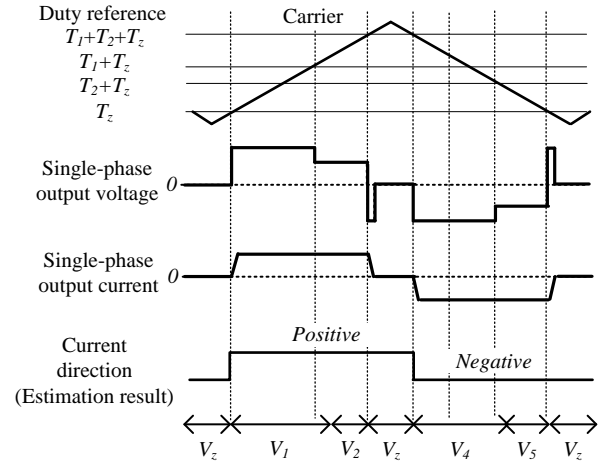


Fig. 7. Estimation principle of current direction. The output current is synchronized the switching carrier by SVM. Therefore, the output current direction is also same relationship.

$$T_z = 1 - (T_1 + T_2) \left(\because |A| = \begin{vmatrix} V_{1\alpha} & V_{2\alpha} \\ V_{1\beta} & V_{2\beta} \end{vmatrix} \right) \quad (5)$$

where v_α and v_β are α - β components of the input current reference, $v_{1\alpha}$, $v_{1\beta}$, $v_{2\alpha}$ and $v_{2\beta}$ are also α - β components of the vectors V_1 and V_2 which are selected based on the area located the input current

Table I. Switching table for two-step commutation.

Sector	I			II			III			IV			V			VI		
Vector	V ₁	V ₂	V _z	V ₂	V ₃	V _z	V ₃	V ₄	V _z	V ₄	V ₅	V _z	V ₅	V ₆	V _z	V ₆	V ₁	V _z
Switching signal	100	010	001	010	010	001	010	001	100	001	001	100	001	100	010	100	100	010
	001	001	100	001	100	010	100	100	010	100	010	001	010	010	001	010	001	100

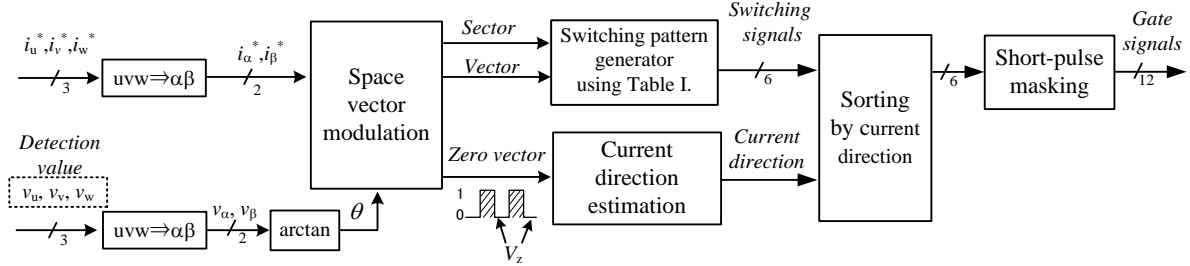


Fig. 8. Signal generation for proposed two-step commutation.

reference.

4.2 Current direction estimation Figure 7 shows the current estimation method to achieve the proposed two-step commutation. The current direction estimation is required for reducing the current sensor which has the high current ratio and the wide bandwidth. The output current is synchronized with the switching carrier by SVM. The switching signal for the zero vector is selected to reduce the output current up to zero. In order to achieve the two-step commutation, the zero current timing at the output side is necessary until end of the zero vector. The output voltage is clamped at the grid voltage during the zero vector when the output current thought via grid voltage. After that, the output current and voltage are also zero. The current direction estimation is achieved to keep the zero current at the output side until end of the zero vector.

4.3 Implementation of proposed two-step commutation

Table I shows the switching table for the proposed two-step commutation. The switching table depends on the sector and the selected output vector. The switching pulse of the same vector is changed by the sector. According to the principle of the proposed two-step commutation as shown in Fig. 3, the gate signals are decided for the six bidirectional switches. For example, the output vector V_1 is selected in the sector I, S_{rp}, S_{sp} and S_{tm} are turned-on. S_{sp}, S_{tm} and S_{sn} are turned-off.

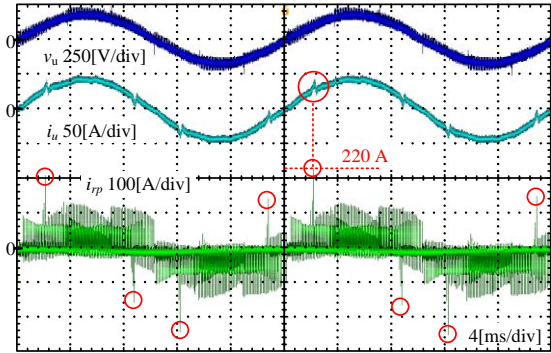
Figure 8 shows the gate signal generation for the proposed two-step commutation which requires the complex commutation algorithm as the four-step commutation because the proposed two-step commutation only uses a switching table and the current direction estimation. The one of two devices in the bi-directional switches is operated by the gate signals depending on the current direction. Another one of that is turned-off during half cycle of the switching frequency. Finally, the short-pulse in the gate signals is masked because the short-pulse wide more than the sum of the raise time and the turn-on delay time required between the switching and next switching on the three-phase to single-phase matrix converter.

5. Experimental results

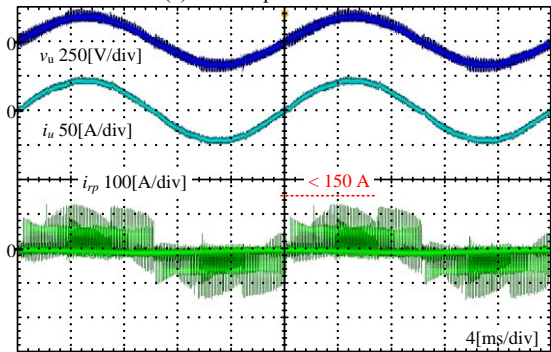
Table II shows the experimental conditions for 10 kW. The switching devices at the three-phase to single-phase matrix converter uses IGBT (MITSUBISHI ELECTRIC: CM400C1Y-24S). The one-step time t_d is decided by the switching characteristics of IGBT. The sum of the raise time and the turn-on delay time of this IGBT is shorter than $1.0 \mu s$. Therefore, the one-

Table II. Experimental condition.

Element	Symbol	Value
Three-phase AC voltage	v_{ac}	200 V
Input frequency	f	50 Hz
Rated output power	P_{out}	10 kW
Carrier frequency	f_c	20 kHz
Turn ratio of transformer	$N_1:N_2$	1:2.4
Input filter	$L_{in} (\%Z)$	350 μH (2.3%)
	$C_{in} (\%Y)$	11 μF (4.7%)
Output filter	L_{out}	1.3 mH
	C_{out}	30 μF
Snubber capacitor	C_s	30 μF
Snubber resistor	R_s	60 k Ω
Commutation time	t_d	1.0 μs



(a) Four-step commutation



(b) Two-step commutation

Fig. 9. Comparison of device current at matrix converter.

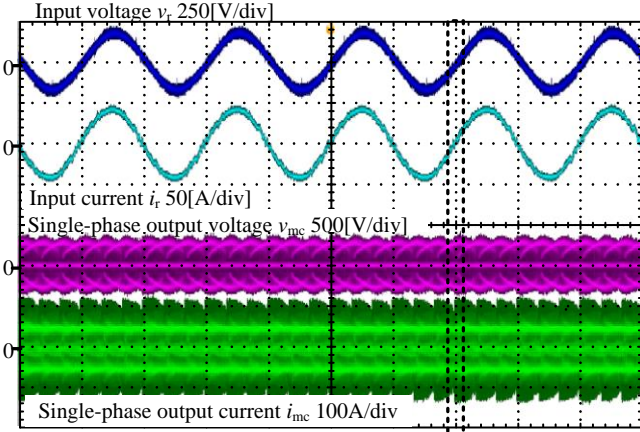


Fig. 10(a) 10[ms/div]

(a) Input and output waveforms of matrix converter

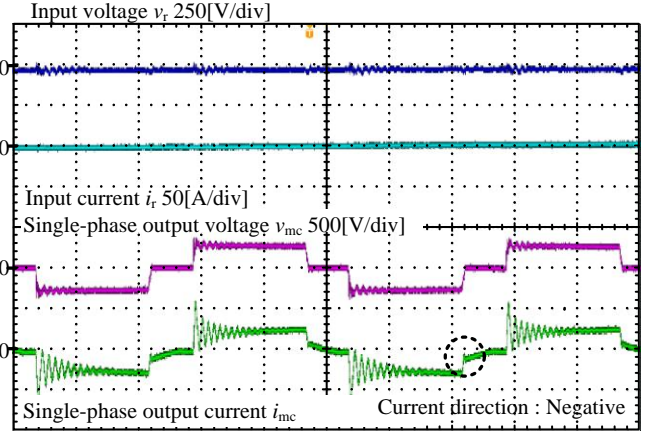


Fig. 10(b) 10[μs/div]

(b) Extended Fig 10(a)

Fig. 10. Four-step voltage commutation with high modulation index (MI = 0.85) at rated power 10 kW.

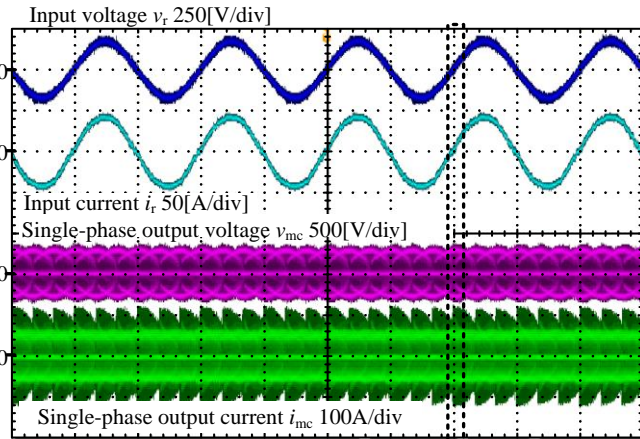


Fig. 11(a) 10[ms/div]

(a) Input and output waveforms of matrix converter

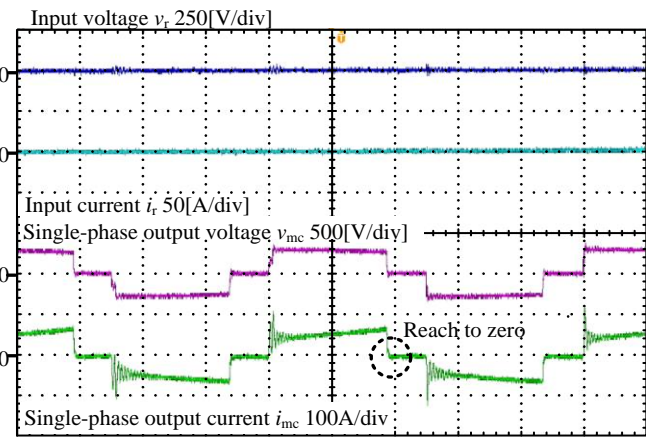


Fig. 11(b) 10[μs/div]

(b) Extended Fig11(a)

Fig. 11. Proposed two-step voltage commutation with high modulation index (MI = 0.85) at rated power 10 kW.

step time sets to 1.0 μs.

Figure 9 (a), (b) shows the experimental waveforms of the three-phase to single-phase matrix converter at 10 kW with the four-step commutation method based on the grid voltage polarity (voltage commutation) and with the proposed two-step commutation method respectively. The commutation failure applying the voltage commutation occurs in the regions where the relationship of the grid voltages changes. As a result, the surge current is approximately 220 A. Consequently, the life time and the reliability of the switching devices is decreased. In addition, the input current is distorted by the commutation failure. The proposed method based on estimation of the output current direction achieves to avoid short-circuit at the grid voltage. Consequently, the input current distortion is low value by 2.9%. In addition, surge current is always suppressed by the proposed two-step commutation.

Figure 10(a)-(b) show the experimental waveforms with the four-step voltage commutation, and the extended waveforms at high modulation index, respectively. The input current has low THD by 4.9% and high-power factor as 0.99. However, the output current does not zero at zero vector.

Figure 11(a)-(b) show the experimental waveforms with the proposed two-step commutation, and the extended waveforms at high modulation index, respectively. It is clear that the output

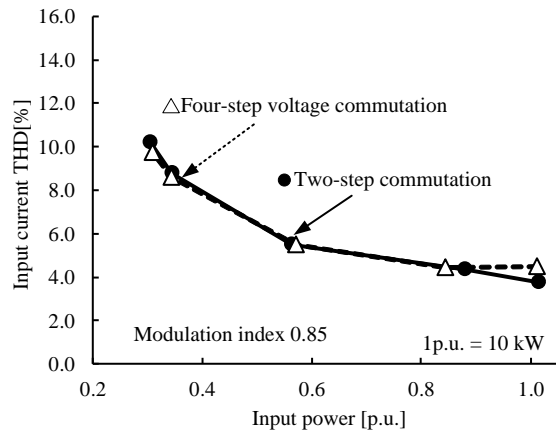
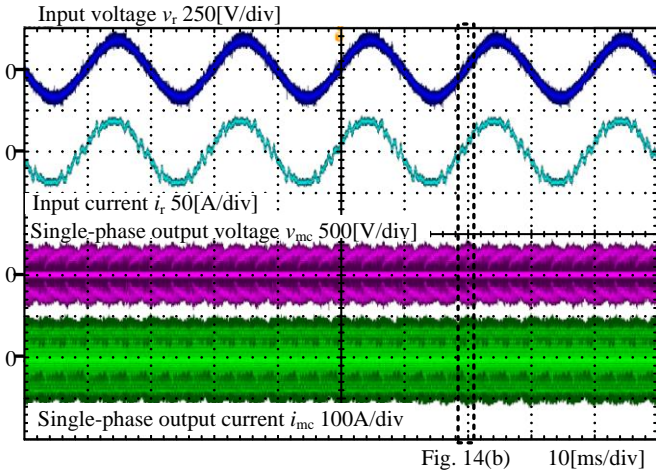


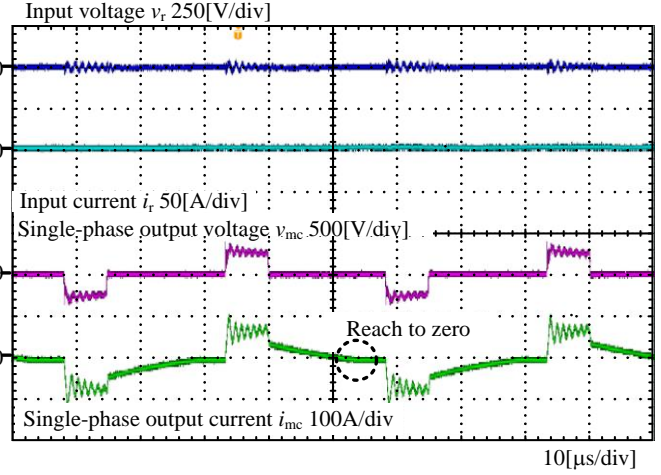
Fig. 12. Comparison of grid current THD at high modulation index. The input current THDs of the proposed two-step commutation and the conventional four-step commutation are also same.

current at the zero vector state quickly decreases to zero. Therefore, the surge voltage due to the output current does not occur when all switches turn-off. It confirms from this result that the proposed two-

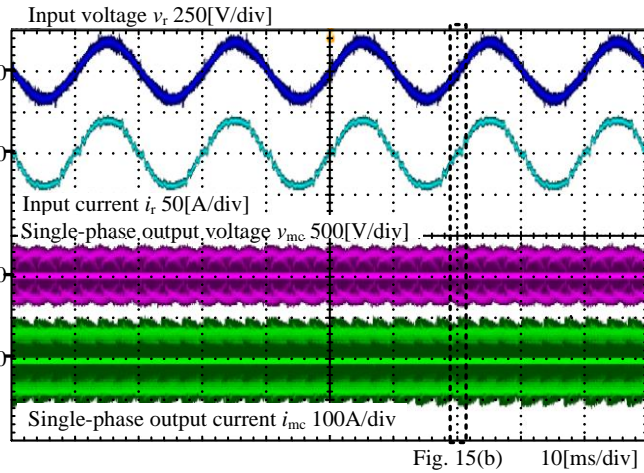


(b) Input and output waveforms of matrix converter

Fig. 13. Four-step voltage commutation with high modulation index (MI = 0.30) at rated power 10 kW.

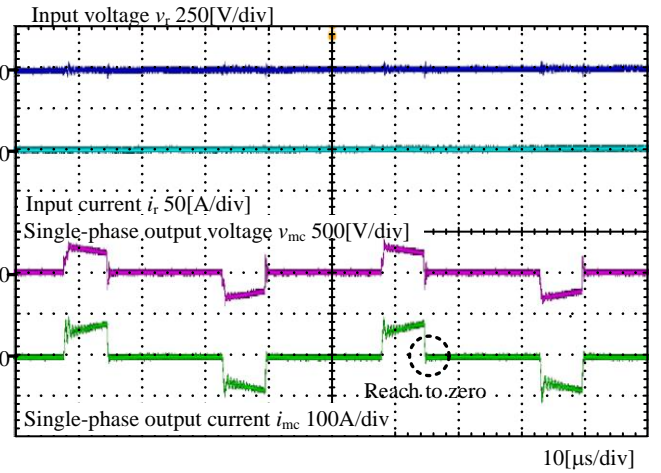


(b) Extended Fig 14(a)



(b) Input and output waveforms of matrix converter

Fig. 14. Proposed two-step voltage commutation with high modulation index (MI = 0.30) at rated power 10 kW.



(b) Extended Fig 14(a)

step commutation method operates the matrix converter without any commutation failures regardless of the input voltage detection error.

Figure 12 shows the characteristics of the input current THD with each commutation method at the high modulation index. The input current THD of the proposed two-step commutation is similar to one of the conventional four-step commutation. The commutation step is decreased by the proposed two-step commutation to keep the performance of input current control.

Figure 13(a)-(b) show the experimental waveforms with the conventional four-step voltage commutation, and the extended waveforms at low modulation index, respectively. The input current is distorted by the masking of the short-pulse.

Figure 14(a)-(b) show the experimental waveforms with the proposed commutation, and the extended waveforms at low modulation index, respectively. It confirms from this result that the proposed two-step commutation method operates the matrix converter regardless of the modulation index.

Figure 15 shows the distortion characteristics of each commutation methods at the low modulation index. The input current THD of the proposed two-step commutation is 7.7% at 10 kW. In the low modulation index, the proposed two-step commutation has the high performance in comparison with the

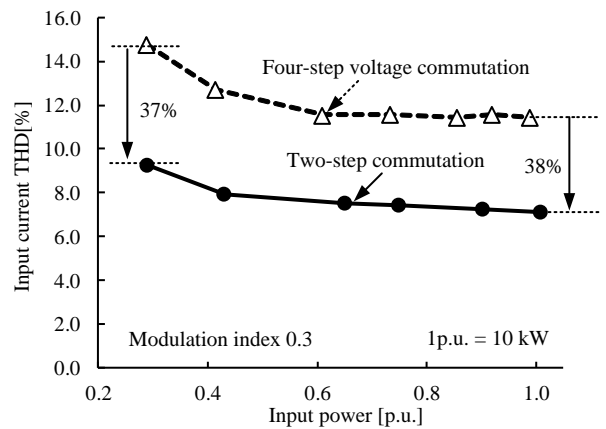


Fig. 15. Comparison of grid current THD with each commutation method at low modulation index. The input current THD is improved by 37 % with the proposed two-step commutation in comparison with the conventional four-step commutation.

conventional four-step commutation at entire loads.

Figure 16 shows the output voltage error of each commutation method. The output voltage error is less than 0.4% regardless of the

modulation index. It is clear that the proposed two-step commutation method is unnecessary to compensate the output voltage error.

Figure 17 shows the distortion characteristics of each commutation methods against the modulation index at rated 10 kW. The input current THD of the proposed two-step commutation is 7.7% at 10 kW. The output voltage range is extended by 36% in case of same input current THD.

Figure 18 shows the efficiency characteristics of each commutation methods. The efficiency characteristics with the conventional four-step voltage commutation and proposed two-step commutation are almost same. It is clear that the switching loss of the matrix converter is not increased to improve the input current THD by applying the proposed commutation.

6. Conclusions

In this paper, the two-step commutation was proposed in the three-phase to single-phase matrix converter. Compared to the conventional two-step commutation, the proposed two-step commutation is always the safety operation regardless of the voltage detection error. In addition, the commutation algorithm of the proposed two-step commutation is much simpler than the conventional commutation. On the other words, the simple control hardware is employed for the matrix converter with the proposed two-step commutation. The input current THD with the proposed two-step commutation is improved by 38% at the low modulation index.

References

- (1) M. Pahlevaninezhad, P. Das, J. Drobnik, P. K. Jain and A. Bakhshai, "A New Control Approach Based on the Differential Flatness Theory for an AC/DC Converter Used in Electric Vehicles," in IEEE Transactions on Power Electronics, vol. 27, no. 4, pp. 2085-2103, April 2012.
- (2) Kohei Aoyama, Naoki Motoi, Yukinori Tsuruta, and Atsuo Kawamura, "High Efficiency Energy Conversion System for Decreases in Electric Vehicle Battery Terminal Voltage", IEEJ Journal of Industry Applications, vol.5, no.1, pp.12-19, 2016.
- (3) S. Kim and F. S. Kang, "Multifunctional Onboard Battery Charger for Plug-in Electric Vehicles," in IEEE Transactions on Industrial Electronics, vol. 62, no. 6, pp. 3460-3472, June 2015.
- (4) Fuka Ikeda, Toshihiko Tanaka, Hiroaki Yamada, and Masayuki Okamoto, "Constant DC-Capacitor Voltage-Control-Based Harmonics Compensation Algorithm of Smart Charger for Electric Vehicles in Single-Phase Three-Wire Distribution Feeders", IEEJ J. Industry Applications, vol.5, no.5, pp.405-406, 2016.
- (5) R. Huang and S. K. Mazumder, "A Soft-Switching Scheme for an Isolated DC/DC Converter With Pulsating DC Output for a Three-Phase High-Frequency-Link PWM Converter," in IEEE Transactions on Power Electronics, vol. 24, no. 10, pp. 2276-2288, Oct. 2009.
- (6) Mahmoud A. Sayed, Kazuma Suzuki, Takaharu Takeshita, Wataru Kitagawa : "PWM Switching Technique for Three-phase Bidirectional Grid-Tie DC-AC-AC Converter with High-Frequency", IEEE Transactions on Power Electronics, 2016
- (7) R. Garcia-Gil, J. M. Espi, E. J. Dede and E. Sanchis-Kilders, "A bidirectional and isolated three-phase rectifier with soft-switching operation," in IEEE Transactions on Industrial Electronics, vol. 52, no. 3, pp. 765-773, June 2005.
- (8) M. A. Sayed; K. Suzuki; T. Takeshita; W. Kitagawa, "PWM Switching Technique for Three-phase Bidirectional Grid-Tie DC-AC-AC Converter with High-Frequency Isolation," in IEEE Transactions on Power Electronics, vol. PP, no.99, pp.1-1
- (9) A. K. Singh; E. Jeyasankar; P. Das; S. Panda, "A Single-Stage Matrix Based Isolated Three Phase AC-DC Converter with Novel Current Commutation," in IEEE Transactions on Transportation Electrification, vol. PP, no.99, pp.1-1
- (10) A. Tajfar and S. K. Mazumder, "Sequence-Based Control of an Isolated DC/AC Matrix Converter," in IEEE Transactions on Power Electronics, vol. 31, no. 2, pp. 1757-1773, Feb. 2016.
- (11) Lixiang Wei, T. A. Lipo and Ho Chan, "Robust voltage commutation of the

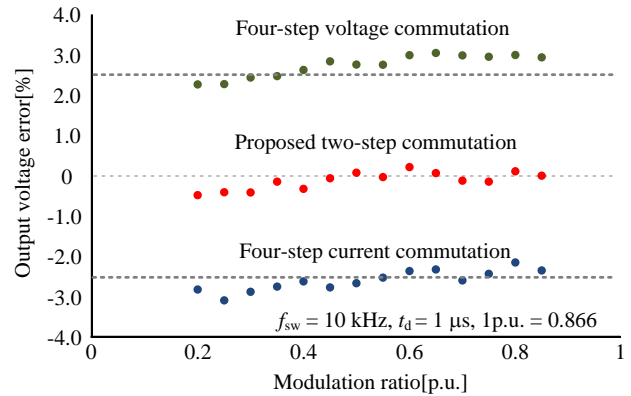


Fig. 16. Comparison of output voltage error.

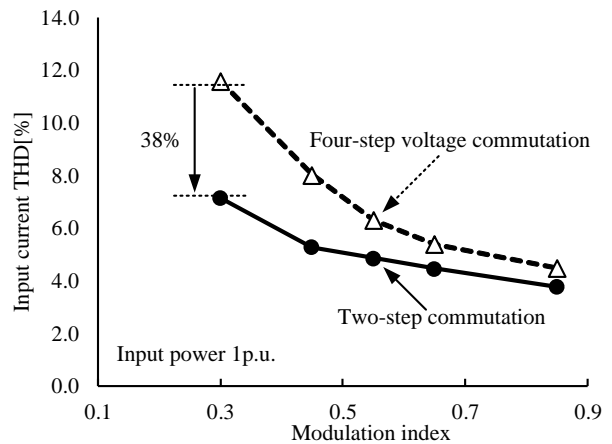


Fig. 17. Comparison of grid current THD with each commutation method at entire modulation index.

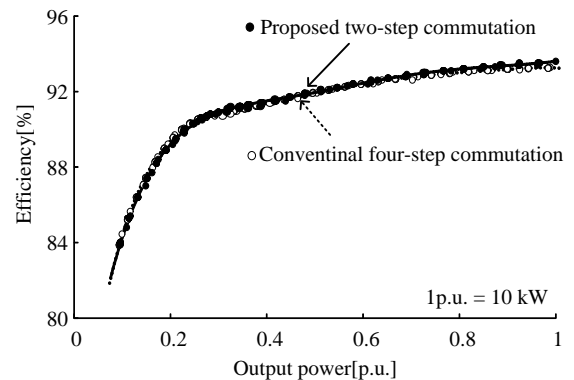
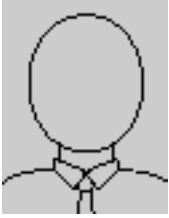


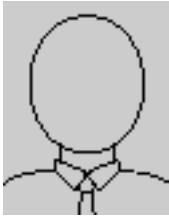
Fig. 18. Comparison of efficiency characteristic with each commutation method.

- (12) T. Schulte and G. Schröder, "Power loss comparison of different matrix converter commutation strategies," 2012 15th International Power Electronics and Motion Control Conference (EPE/PEMC), Novi Sad, 2012, pp. DS2c.9-1-DS2c.9-6.
- (13) S. Tamaruckwattana, Chenxin Yue, Y. Ikeda and K. Ohya, "Comparison of switching losses of matrix converters for commutation methods," 2014 16th European Conference on Power Electronics and Applications, Lappeenranta, 2014, pp. 1-10.

Shunsuke Takuma (Student member) received his B.S. degree in science of technology innovation from Nagaoka University of Technology, Niigata, Japan in 2015. Presently, he is a Ph.D. candidate at Nagaoka University of Technology, Niigata, Japan. He is the student member of IEEJ and IEEE. His current research interests include commutation techniques and the implement of the matrix converter.



Jun-ichi Itoh (Senior member) received his M.S. and Ph.D. degree in electrical and electronic systems engineering from Nagaoka University of Technology, Niigata, Japan in 1996, 2000, respectively. From 1996 to 2004, he was with Fuji Electric Corporate Research and Development Ltd., Tokyo, Japan. He was with Nagaoka University of Technology, Niigata, Japan as an associate professor. Since 2017, he has been a professor. His research



interests are matrix converters, dc/dc converters, power factor correction techniques, energy storage system and adjustable speed drive systems. He received IEEJ Academic Promotion Award (IEEJ Technical Development Award) in 2007. In addition, he also received Isao Takahashi Power Electronics Award in IPEC-Sapporo 2010 from IEEJ, 58th OHM Technology Award from The Foundation for Electrical Science and Engineering, November, 2011, Intelligent Cosmos Award from Intelligent Cosmos Foundation for the Promotion of Science, May, 2012, and Third prize award from Energy Conversion Congress and Exposition-Asia, June, 2013. Prizes for Science and Technology (Development Category) from the Commendation for Science and Technology by the Minister of Education, Culture, Sports, Science and Technology, April 2017. He is a senior member of the Institute of Electrical Engineers of Japan, the Society of Automotive Engineers of Japan and the IEEE.